Applied Catalysis B: Environmental 90 (2009) 205–212

Contents lists available at ScienceDirect

Applied Catalysis B: Environmental

journal homepage: www.elsevier.com/locate/apcatb

Deposition of TiO_2 and Ag:TiO_2 thin films by the polymeric precursor method and their application in the photodegradation of textile dyes

Andréa R. Malagutti [a], Henrique A.J.L. Mourão [a,b], José R. Garbin [a,c], Caue Ribeiro [a,*]

[a] Embrapa Instrumentação Agropecuária, Rua XV de Novembro 1452, CEP 13560-560, CP 741, São Carlos, SP, Brazil
[b] Departamento de Química da Universidade Federal de São Carlos, Rod. Washington Luiz km 235, CEP 13565-905, São Carlos, SP, Brazil
[c] Natureza Ativa Indústria e Comércio de Fotoreator Ltda ME, NATV, Rua Alfredo Lopes, 1717, São Carlos, SP, Brazil

ARTICLE INFO

Article history:
Received 13 November 2008
Received in revised form 5 February 2009
Accepted 6 March 2009
Available online 19 March 2009

Keywords:
Thin films
Titanium dioxide
Photodegradation
Rhodamine B

ABSTRACT

This paper describes the development of nanostructured thin films of TiO_2 and Ag:TiO_2 with different Ag loading content and with various number of layers by the polymeric precursor method, in order to test them in the photocatalysis of the degradation of textile dyes, using rhodamine B as a standard. Analysis of the films showed that the adopted method could be used to synthesize pure anatase and the silver-decorated phase. Moreover, 0.25% Ag:TiO_2 thin film showed enhanced photocatalytic efficiency. The tests with film of different thickness showed that for pure TiO_2, the increase in film thickness was the only factor responsible for improving the photocatalytic activity, whereas for the Ag:TiO_2 thin films, the increase in photocatalytic activity was related to associate effects: the electron transfer from TiO_2 to Ag, reducing the electron–hole recombination, and the increase in film thickness.

1. Introduction

Semiconductor-mediated photocatalytic oxidation is regarded as a promising method for environmental decontamination. Among the semiconductors employed, TiO_2 is considered a good photocatalyst because of its high photosensitivity, non-toxicity, easy availability, strong oxidizing power and long-term stability [1,2]. This semiconductor occurs in three different crystalline forms, rutile, brookite and anatase, the last of these having remarkable photocatalytic activity [3]. Thus, nanoparticles of the semiconductor anatase have been under intense investigation for possible application in the removal of organic contaminants from air and water [4–8].

In the literature, several reports have appeared on TiO_2 thin films produced by different techniques. Sayılkan et al. [9] reported the preparation of TiO_2 thin films by thermal hydrolysis. Sankapal et al. [10] described the synthesis of nanocrystalline titanium dioxide thin films and powders by chemical and electrochemical deposition methods. Venkatachalam et al. [2] prepared nanocrystalline TiO_2 photocatalysts of different anatase to rutile ratios by a sol–gel technique. There are large variations in the properties of TiO_2 thin films produced by each technique. However, the production of anatase TiO_2 phase is not trivial, and represents an interesting case where synthesis of TiO_2 on the nanometric scale favors the anatase phase over rutile [11]. Thus, synthesis methods able to control the final particle size are necessary for development of the phase [12,13].

An interesting method of controlling the size and the surface contamination of TiO_2 nanoparticles obtained by calcination is the polymeric precursor method [14]. This method is based on the ability of polycarboxylic acids, particularly citric acid (CA), to form very stable water-soluble complexes that can be polymerized by polyesterification with a polyalcohol, to form a resin. This process leads to the formation of a polymeric precursor with the cations homogeneously distributed in a three-dimensional solid lattice, avoiding precipitation or phase separation during the synthesis of the metal oxide [14]. It is known to be suitable for the formation of thin films by deposition of the polymeric resin on a substrate and calcination of this specimen leading to the *in situ* formation of the oxide film. This is also a possible method for the immobilization of photocatalyst and its use in photo-reactors [14].

However, one of the main challenges to optimizing TiO_2 nanostructures is the high rate of recombination of the electron–hole pairs, which reduces significantly the photocatalytic efficiency. A reduction in the recombination rate and consequent increase in the efficiency can be achieved by the incorporation of noble metal into the structure of the semiconductor [15]. There have been several reports on metal incorporation to inhibit the recombination processes [16,17]. Anpo and Takeuchi [18] showed that the incorporation of small amounts of Pt in the TiO_2 structure dramatically increases the photocatalytic activity of the semiconductor, because the metal centers enhance the charge

* Corresponding author. Tel.: +55 16 2107 2800; fax: +55 16 2107 2902.
E-mail address: caue@cnpdia.embrapa.br (C. Ribeiro).

0926-3373/$ – see front matter © 2009 Elsevier B.V. All rights reserved.
doi:10.1016/j.apcatb.2009.03.014

separation of the electrons and holes generated by light irradiation. Wang et al. [19] also reported the increase of photocatalytic efficiency of mesoporous anatase TiO_2 powders of high surface area by the incorporation of Ag nanoparticles. However, at the moment, the photocatalytic activity of thin films obtained by the polymeric precursor method, doped or otherwise, has been investigated little.

Hence, this paper reports the synthesis of pure TiO_2 and with different Ag loading content Ag:TiO_2 nanostructured thin films and with various number of layers by the polymeric precursor method. The photocatalytic activity of the thin films was assessed by degradation of rhodamine B in aqueous solution under UV illumination, used here as a model textile dye. The results presented here may assist in the understanding of the phenomena involved in the photocatalytic degradation of pollutants using immobilized materials supported as thin films.

2. Experimental

Ti^{4+} resins were prepared by the polymeric precursor method. The method consists in dissolving titanium tetraisopropoxide (Aldrich) in an aqueous solution of citric acid (Merck), at 75 °C in a molar ratio of 1:3. After complete dissolution and homogenization by magnetic stirring, the titanium citrate obtained was polymerized by adding ethylene glycol (Merck). Ag^+ resins were obtained in the same way, but with silver nitrate as precursor salt.

Pure TiO_2, Ag:TiO_2 (0.25; 0.50 and 1.0 wt% Ag) and pure Ag thin films were prepared on glass substrates, the Ag film being used to compare and identify the related effects of pure Ag, as a possible distinct phase in the Ag:TiO_2 thin films. The glass substrates (2.5 cm × 2.5 cm, borosilicate glass) were first cleaned in a mixture of 3:1 H_2SO_4 (Merck), and with 30% H_2O_2 (v/v) (Synth), followed by a mixture of sodium hydroxide (Merck) and hydrogen peroxide solution, to hydrophilize the glass substrate surface. The resins were deposited on the glass substrates by the spin-coating technique, with an initial rotation speed of 1000 rpm for 10 s, followed by 5000 rpm for 40 s. The thin films were firstly heat-treated at 300 °C in a conventional electric oven for 2 h, to promote pyrolysis of the resin, resulting in an amorphous film, and later crystallized at 450 °C, 2 h, to form the nanometric film.

Due to the poor resolution obtained in X-ray diffraction (XRD) experiments directly in the films, the XRD analysis were done in powders obtained in the same procedure used to produce the films. Pure TiO_2, 1.0% Ag:TiO_2 and pure Ag powder samples were obtained by adding 0.5 mL of the each previously prepared resin in porcelain crucibles, and after the resins were heat-treated at 300 °C in a conventional electric oven for 2 h and later crystallized at 450 °C for 2 h to form the nanometric powder.

The titanium oxide thin films were characterized by Raman spectroscopy (FT Raman Bruker RFS 100/S), using the 1064 nm line of a 450 W YAG laser, and 200 scans for each measure at room temperature. The X-ray diffraction spectra were collected with a Rigaku diffractometer model Dmax 2500 PC, with a Cu ($\lambda_{Cu\text{-}k\alpha}$ = 1.5418 Å) anode. The morphology of the thin films was observed by atomic force microscopy (AFM NanosScope IIIA Veeco NanoMan).

Diffuse reflectance UV–vis spectra (DRS) were obtained using an ultraviolet–visible–near infrared (UV–vis–NIR) Cary 5G spectrophotometer. The spectrum of the substrate was taken as baseline and the baseline correction procedure was executed prior to each measurement. UV–vis spectra were performed in the diffuse reflectance mode (R) and transformed to a magnitude proportional to the extinction coefficient (K) through the Kubelka–Munk model that relates the extinction coefficient and the scattering (S) with the reflectance, in agreement with the Eq. (1). For comparison, all spectra were arbitrary normalized in intensity to 1.0.

$$\frac{K}{S} = \frac{(1-R)^2}{2R} \quad (1)$$

Similarly to the XRD analysis, the X-ray photoelectron spectroscopy (XPS) showed poor resolution when performed directly in the films, and the analysis was only possible when done in powders obtained in the same procedure used to produce the films The XPS analysis was carried out using a commercial spectrometer (UNI-SPECS UHV). The Mg Kα line was used (E = 1253.6 eV) and the analyzer pass energy was set to 10 eV. The inelastic background of the C 1s, Ti 2p, O 1s and Ag 3d electron core-level spectra was subtracted using Shirley's method. The binding energies of the spectra were corrected using the hydrocarbon component of the polymer fixed at 285.0 eV. The composition of the surface layer was determined from the ratio of the relative peak areas corrected by sensitivity factors of the corresponding elements. The spectra were fitted without placing constraints using multiple Voigt profiles. The width at half maximum (FWHM) varied between 1.6 and 2.0 eV and the accuracy of the peak positions was ±0.1 eV.

Square wave voltammetry measurements were performed in a conventional electrochemical cell with a three-electrode system, using an Autolab-PGZ 30 potentiostat/galvanostat. A pure TiO_2 film, pure Ag film and 1.0% Ag:TiO_2 film deposited on a titanium substrate with various number of layers served as working electrodes; and an Ag/AgCl electrode and a platinum sheet (30 mm × 30 mm) served as reference and counter electrode, respectively. A 0.5 mol L^{-1} NaCl aqueous solution was employed as a supporting electrolyte. All the electrochemical measurements were carried out without illumination at room temperature.

The photocatalytic activity of the films for the oxidation of rhodamine B (RhoB) was tested under UVC illumination. The thin films with various layers deposited on glass substrates (same substrate area) were placed in beakers, immersed in 20 mL of an aqueous solution of rhodamine B (2.5 mg L^{-1}). The beakers were placed in a photo-reactor at 25 °C and illuminated by four UVC lamps (TUV Philips, 15 W, maximum intensity at 254 nm). The photocatalytic oxidation of RhoB was monitored by taking UV–vis measurements (Shimadzu-UV-1601 PC spectrophotometer) various times of light exposure.

3. Results and discussions

3.1. Photocatalyst characterization

XRD analyses of the thin films were done, but, owing to their small thickness, it was not possible to identify the phases correctly. Therefore, powder patterns were prepared from samples of the same resins subjected to the same heat treatment, as shown in Fig. 1. It was possible to detect the presence of the rutile phase in the TiO_2 powder, in a small amount compared to the anatase phase. The Ag doping favored anatase phase stabilization, since the rutile phase peaks practically disappeared in the 1.0% Ag:TiO_2 samples. In the Ag powder, only metallic Ag was observed.

To evaluate the presence of the desired phases in the freshly prepared films, the Raman spectra of four-layered samples were recorded, as shown in Fig. 2 for the glass support (a), pure Ag film (b), pure TiO_2 film (c) and 1.0% Ag:TiO_2 film (d). The anatase TiO_2 phase could be identified by the major Raman band at 144 cm^{-1} (the strongest for anatase), attributed to the Raman-active mode with the symmetries of E_g [20]. Thus is confirmed that the adopted method of synthesis leads to the formation of the desired anatase phase in the thin films. Moreover, no sign of rutile TiO_2 was detected (intense line at 445 cm^{-1}). In the case of the pure Ag film, no phase was identified, as expected for metals. The difficulty in identifying the phases using

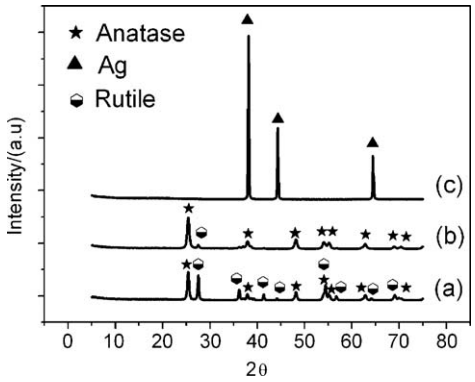

Fig. 1. The XRD powder patterns of (a) pure TiO_2; (b) 1.0% Ag:TiO_2 and (c) pure Ag.

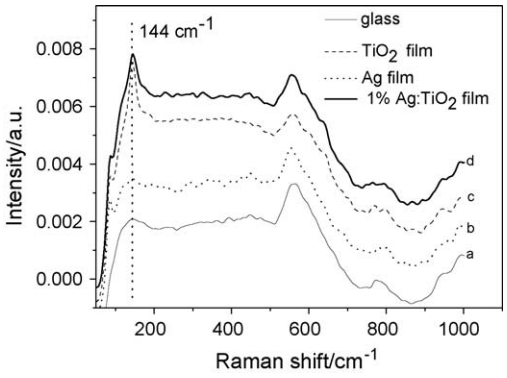

Fig. 2. Raman spectra of TiO_2, Ag and 1.0% Ag:TiO_2 thin films with four layers.

Raman spectroscopy was due to the synthesized materials being nanostructured thin films, which posses very little thickness, so that the scattering of radiation is very weak and the signal/noise ratio is low. Comparing these results with the XRD patterns (Fig. 1), it can be concluded that the immobilization of the Ti-containing resin as a thin film also favored anatase phase stabilization. Thus, the deposition of the photocatalyst as a thin film and the Ag doping were both advantageous, since the anatase phase is the most photoactive among the TiO_2 phases.

Fig. 3 shows the AFM images for the TiO_2, Ag and 1.0% Ag:TiO_2 thin films. As shown in this figure, continuous and regular films were formed, without a significant change in morphology in the doped film, suggesting that the 1.0% Ag:TiO_2 film sample did not undergo phase separation, in agreement with the XRD patterns (Fig. 1). According to the roughness values shown in Table 1, increasing thickness of either pure TiO_2 or pure Ag thin films leads to a small increase in roughness, whereas for the 1.0% Ag:TiO_2 thin film, there was a reduction in the roughness of the film with increasing thickness. However, the roughness variation among these values may be considered random, and a specific contribution of Ag doping to the roughness cannot be defined. This fact indicates that the method used is sufficiently

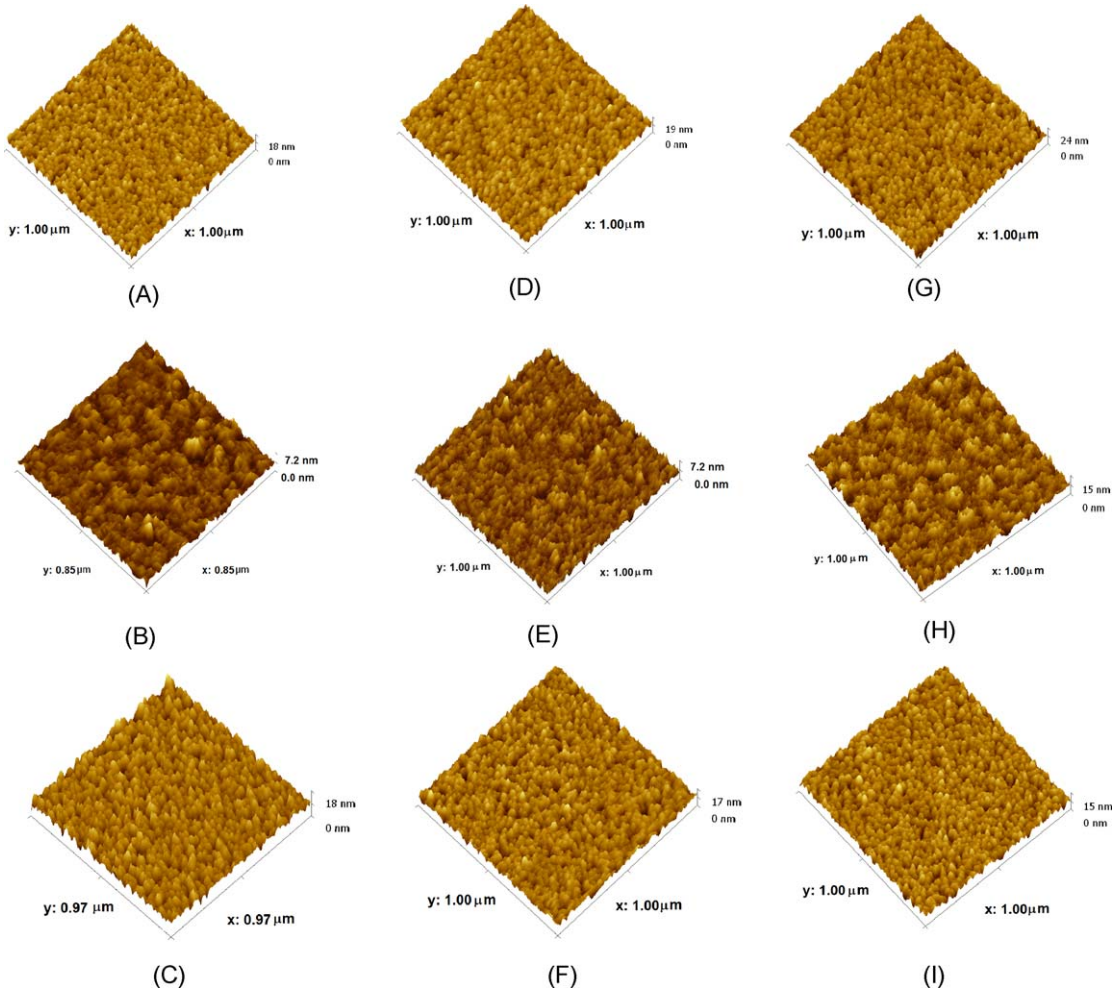

Fig. 3. AFM images showing the thin film surfaces with different number of layers of TiO_2: (A) monolayer; (D) two layers; (G) four layers; of Ag; (B) monolayer, (E) two layers; (H) four layers and 1.0% Ag:TiO_2; (C) monolayer; (F) two layers and (I) four layers.

Table 1
Roughness of TiO_2, Ag and 1.0% Ag:TiO_2 films measured by AFM.

Film	Roughness (nm)		
	TiO_2	Ag	1% Ag:TiO_2
Monolayer	1.70	0.79	1.88
Two layers	1.69	0.71	1.73
Four layers	2.23	1.79	1.63

reproducible in relation to the degree of covering and the presence of doping.

Fig. 4 shows the optical absorption spectra of the prepared samples. In Fig. 4A, it can be seen that for pure TiO_2 film, the band gap value corresponds to 3.4 eV (onset at 360 nm), near to the expected value for the material [18]. The presence of pure Ag in the film would lead to a totally opaque system in this region, but, a transition can be seen at 300 nm (4.1 eV), which is probably related

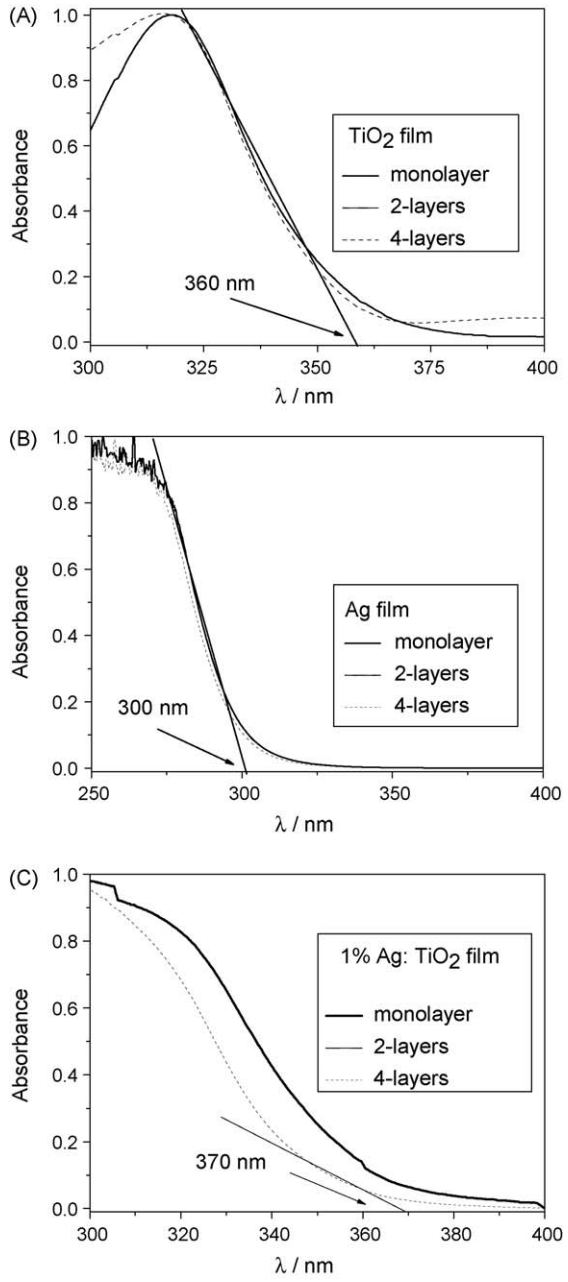

Fig. 4. Optical absorption spectra of (A) TiO_2; (B) Ag and (C) 1.0% Ag:TiO_2 thin films.

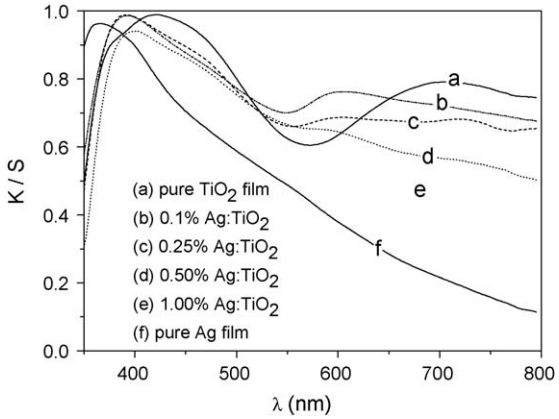

Fig. 5. Diffuse reflectance spectra for two layers of (a) pure TiO_2 film; of Ag-doped TiO_2 film with (b) Ag:TiO_2 (0.10%); (c) Ag:TiO_2 (0.25%); (d) Ag:TiO_2 (0.50%); (e) Ag:TiO_2 (1.0%) and of (f) pure Ag film.

to the glass substrate. Since the film is very thin, it remains transparent. When TiO_2 is doped with the noble metal, the result is a displacement of the absorption band towards the visible region of the absorption spectra, with an onset at 370 nm (3.3 eV). This small reduction in the band gap can interfere with the absorption of photons. One can also see in Fig. 4C a widening of the absorption band in the 1.0% Ag:TiO_2 film, indicating an increase in the number of possible electron transitions, confirming the effective doping of the film. Thus, it is possible to conclude that the change of the onset between TiO_2 and 1.0% Ag:TiO_2 is not a result of adding the individual absorption profiles of TiO_2 and Ag.

Fig. 5 presents the diffuse reflectance spectra for the two layers of pure Ag film, of pure TiO_2 film and of Ag:TiO_2 films with different Ag content. It can be seen that the spectra of TiO_2 film was different from pure Ag and Ag:TiO_2 composite thin films. The peaks observed at around 380–400 nm for the Ag film and for all Ag:TiO_2 films can be attributed to the plasmon peak of Ag spherical nanoparticles at 400 nm [21,22]. The surface plasmon absorption band of metal nanoparticles can be influenced by many factors such as particle size, particle shape, particle size distribution, surface charge density etc. Also, the surface plasmon absorption peak became broader and moved to longer wavelengths when the size of nanoparticle increased. The increase in size distribution also led to broadening of the surface plasmon absorption peak [21]. It can be seen from Fig. 5 that the surface plasmon absorption peak became broader with the increasing of Ag content. This suggests that the Ag nanoparticle size distribution became wide with increasing of Ag content. However, since in all samples the plasmon effect is relatively low, it can be considered that this effect is not very significant to the overall behavior of the material as a photocatalyst.

The valence state of Ag was observed by XPS measurement. Fig. 6, shows the high-resolution XPS spectra of: (A) Ti 2p region for 1.0% Ag:TiO_2 powder. The 2p region shows a main peak at binding energy of 458.6 eV that was attributed to the TiO_2; (B) O 1s region for 1.0% Ag:TiO_2 powder. The O 1s regions could be fitted into two peaks. The main peak at a binding energy of 530.0 eV was attributed to the Ti–O in TiO_2. The minor peak was due to the hydroxyl group. The hydroxyl on the surface can be attributed to the Ti–OH on the powder; and (C) Ag in the 1.0% Ag:TiO_2 powder. The Ag $3d_{5/2}$ peak appeared at a binding energy of 368.1 eV. This binding energy indicated that silver was of metallic nature [21]. This indicated that metallic Ag nanoparticles were introduced to TiO_2 powder, and a real doping of the nanoparticles did not occur. In fact, one can affirm that the silver nanoparticles are probably decorating the surface of TiO_2 nanoparticles, forming a nanocomposite.

The same result was observed by square wave voltammetry measurements performed in the films, where we observed the

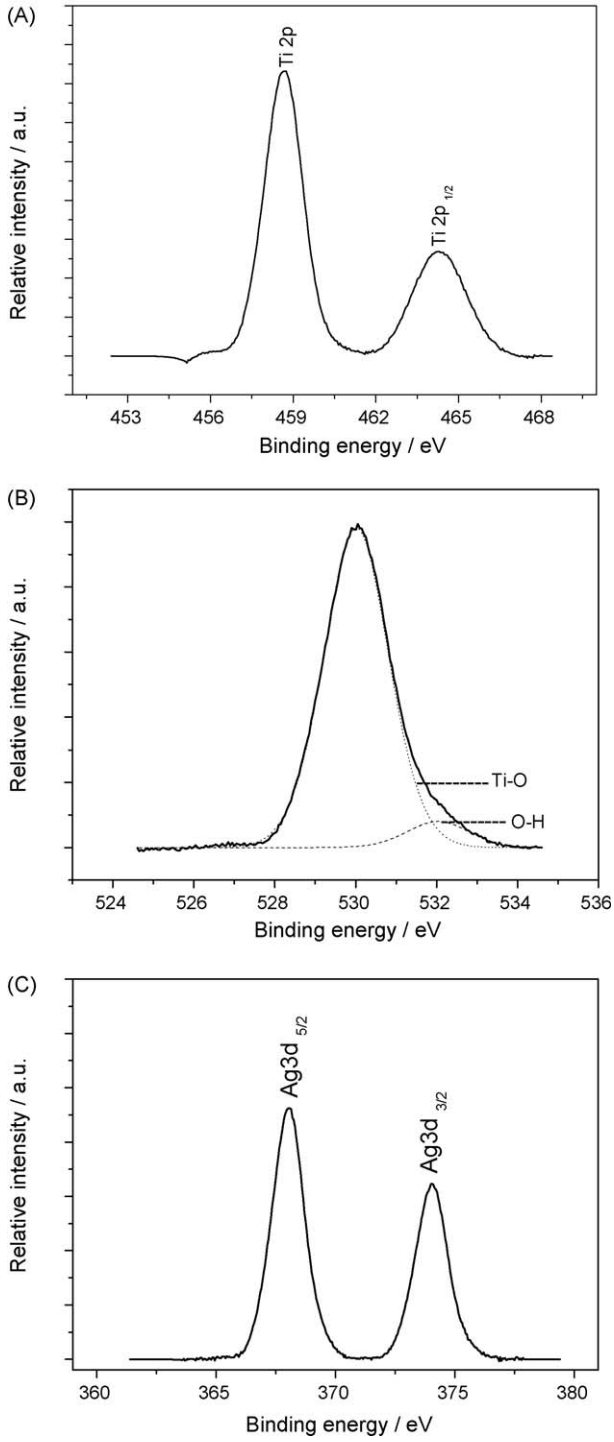

Fig. 6. High-resolution XPS spectra of (A) Ti 2p region for 1.0% Ag:TiO_2 powder; (B) O 1s region for 1.0% Ag:TiO_2 powder and (C) Ag in 1.0% Ag:TiO_2 powder.

presence of an oxidation peak at 0.07 V (versus Ag/AgCl) in the voltammetric profiles of the pure Ag film and of the 1.0% Ag:TiO_2 film with various numbers of layers, as shown in Fig. 7. This indicated the existence of metal Ag with its valence state being Ag^0, that was oxidized electrochemically to Ag^+ in the pure Ag and 1.0% Ag:TiO_2 films surfaces.

3.2. Assays of RhoB degradation catalyzed by nanostructured films

When a photon incident on a semiconductor has energy hc/λ that matches or exceeds the bandgap energy (E_{bg}) of the

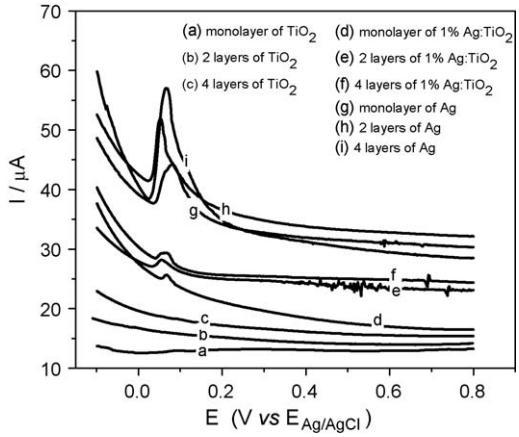

Fig. 7. Square wave voltammograms for the monolayer, two layers and four layers of pure TiO_2, of pure Ag and of 1.0% Ag:TiO_2 thin films in 0.5 mol L^{-1} NaCl aqueous solution without UV illumination, at scan increment (ΔE_s) of 2 mV, pulse amplitude (ΔE_p) of 50 mV and frequency (f) of 10 Hz.

semiconductor, an electron (e^-) is promoted from the valence band, VB, into the conduction band, CB, leaving a hole (h^+) in the valence band. Excited-state CB electrons and VB holes can recombine and dissipate the input energy as heat, get trapped in metastable surface states, or react, respectively, with electron acceptors and donors that happen to be adsorbed on the semiconductor surface or within the surrounding electrical double layer of the charged nanoparticles. In the absence of suitable e^-/h^+ scavengers the stored energy is dissipated within a few nanoseconds by recombination. If a suitable scavenger or surface defect state is available to trap the electron or hole, recombination is prevented and subsequent redox reactions may occur [23].

In the thin films in question, the photocatalytic oxidative activity resides in the surface h^+ and, thus, the conduction of electrons into bulk material is necessary to prevent recombination. In films deposited on an insulating support (glass, for example), the electrons can be displaced to lower layers of the films but, since their transfer to the insulating support is not possible, they are confined in the film and may recombine (Fig. 8). Thus, the effects of the thickness of the film and the Ag doping of the TiO_2 on the photocatalytic efficiency of the synthesized films were investigated.

As already reported, the Ag loading content has an important effect on the photocatalytic activity and strong Ag loading may result in a photohole trapping effect. Due to the fact that the Ag particles and clusters on the TiO_2 nanoparticles are relatively negative charged, the photoholes in the interfacial region of the TiO_2 film may be trapped by the negatively charged Ag particles and cluster before they react with water and organics [24]. This effect can decrease the photocatalytic activity. For this reason the effect of the Ag loading content on the photocatalytic degradation of RhoB was investigated, as shown in Fig. 9.

As can be seen in Fig. 9 the photocatalytic activity of Ag:TiO_2 thin films was higher than pure TiO_2. The trapping effect was negligible when the Ag loading content is 0.25% due the high efficiency in the charge separation in the TiO_2 film surface. However, it was observed that the photocatalytic activity of TiO_2 is reduced with the increase of the Ag loading content above of 0.25% in the thin films. The decrease in the photocatalytic activity can be associated with trapping effect and also with the change of the reaction site density. As the Ag^+ concentration increase, the coverage of Ag on TiO_2 surface will increase, and the density of reaction sites for absorption of UV light, producing photohole and photoelectrons at surface of the resulting film would decrease [24].

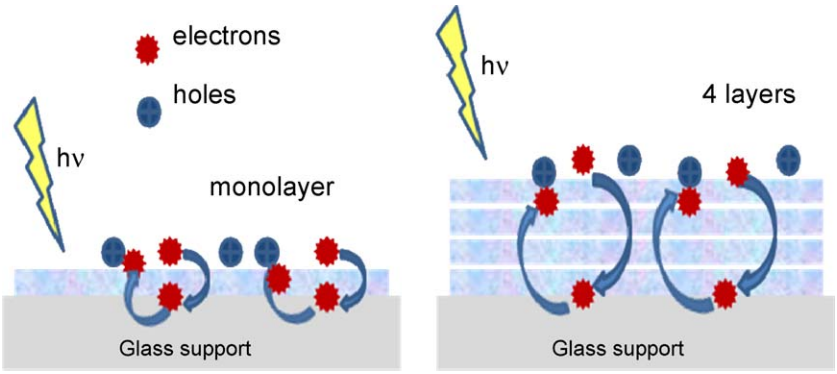

Fig. 8. Scheme of the recombination process with the increase in the number of layers of the TiO_2 film.

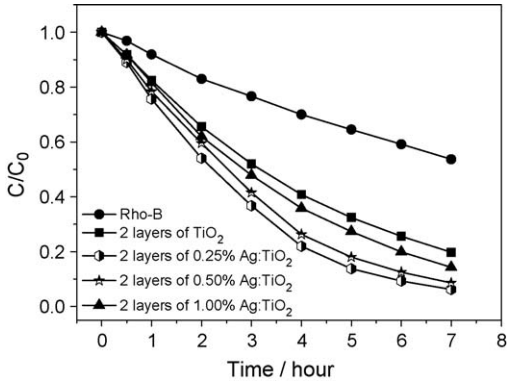

Fig. 9. Photodegradation profiles of the RhoB solution under different percentage of Ag:TiO_2 for the two-layer thin film.

In order to observe the Ag loading effect, including its possible deleterious effects, an analysis of the thickness influence in the photocatalytic activity of the films was done using the higher content studied in this work, 1.0% Ag content. Fig. 10 shows the photodegradation profiles for RhoB solution, with the TiO_2 films (graph A), Ag films (graph B) and 1.0% Ag:TiO_2 films (graph C) with various numbers of layer.

As can be observed in Fig. 10A, for the pure TiO_2 film, the efficiency in degrading RhoB increased with the film thickness. This result can be explained by assuming that in thicker films the electrons can travel further before returning to the surface of the semiconductor, making the recombination process slower and implying higher photocatalytic efficiency, owing to a greater density of h^+ at the surface. In very thin layers, this effect is too fast, due to the shorter electron path, resulting in a lower efficiency. Thus, in the case of the pure TiO_2 film, the photocatalytic activity may increase with thickness. However, in very thick films, other effects related to the opacity of the film may take place, reducing the activity.

In Fig. 10B, it can be seen that an increase in the efficiency of photodegradation by the Ag film occurred for both monolayer and two-layer films, compared to the direct photolysis of the RhoB. However, the four-layer film was ineffective for the photodegradation. In this case, the results suggest that the film is a mixture of Ag and Ag_2O, probably with a higher concentration of the oxide at the surface, due to the calcination method used. Thus, a possible reaction on the Ag films is the reduction of Ag^+ to Ag^0. This reaction would consume photon energy, reducing the part available for the photocatalytic process. In thicker films, the interference of the oxide could be greater. Thus, it can be seen that the Ag film produced by the polymeric precursor method is

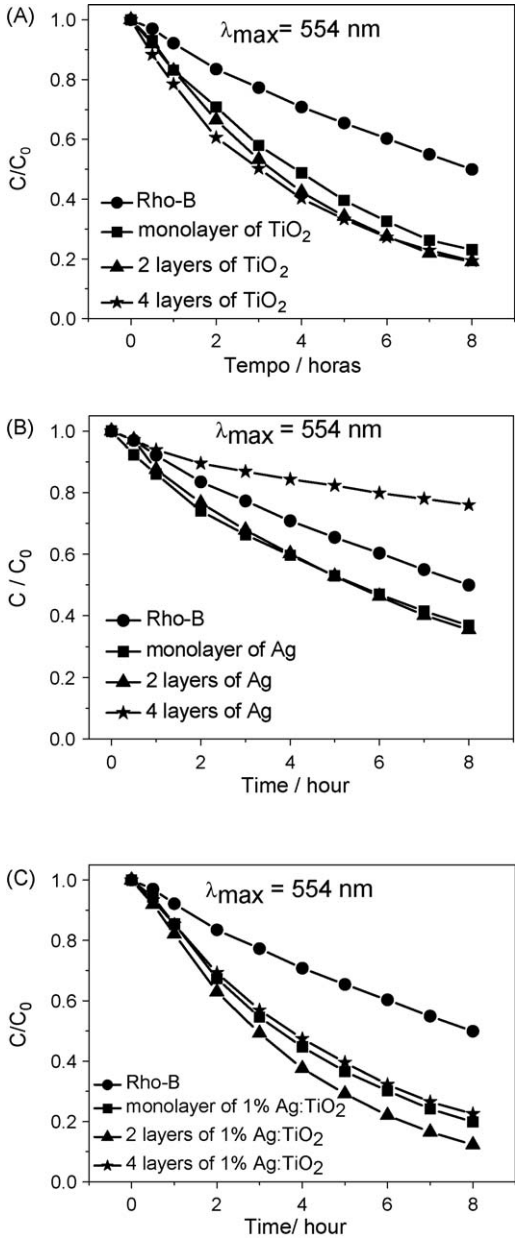

Fig. 10. Photodegradation profiles of the RhoB solution, using films with different number of layers of: (A) TiO_2; (B) Ag and (C) 1.0% Ag:TiO_2 deposited on glass.

not effective in the photocatalytic process under these conditions.

The results of Fig. 10C show that the presence of 1.0% Ag:TiO_2 film increased the efficiency of RhoB photodegradation observed in the absence of photocatalyst. As it can be verified in Fig. 10C, the two-layer 1.0% Ag:TiO_2 film showed higher photocatalytic efficiency than the monolayer and four-layer films. This increase in catalytic efficiency may be attributed to two different effects: electron transfer between TiO_2 and Ag^+ (electron capture) and the increased layer thickness, relative to the monolayer. Both effects may reduce the speed of recombination. However, it was observed that in thicker films, the presence of the Ag^0 made the film cloudy, so that less light was absorbed by the semiconductor and the generation of h^+ and e^- and, consequently, the catalytic activity, were reduced. From these photodegradation results, there is apparently an optimum film thickness, where a balance between the effects of electron capture by Ag and bulk thickness of anatase (which increase photoactivity) and the opacity due to metallic Ag (which reduces the photoactivity) is attained. This optimal result was observed for the film with an intermediate number of layers (two) in the case of 0.25% Ag:TiO_2 as already shown in Fig. 9.

Fig. 11 shows the absorption spectra of RhoB solution after 4 h photodegradation by the two-layer films of Ag, TiO_2 and 1.0% Ag:TiO_2 (Fig. 11A) and also comparative plots of RhoB degradation over 8 h, showing the photocatalytic efficiency of these films (Fig. 11B).

From the plots obtained of the photocatalytic efficiency of the two-layer films of Ag, TiO_2 and Ag:TiO_2 with different percentage of Ag, the order of the photodegradation reaction was calculated.

From the exponential profiles observed in Figs. 9 and 11, the reaction should be first-order with respect to RhoB, and the kinetic

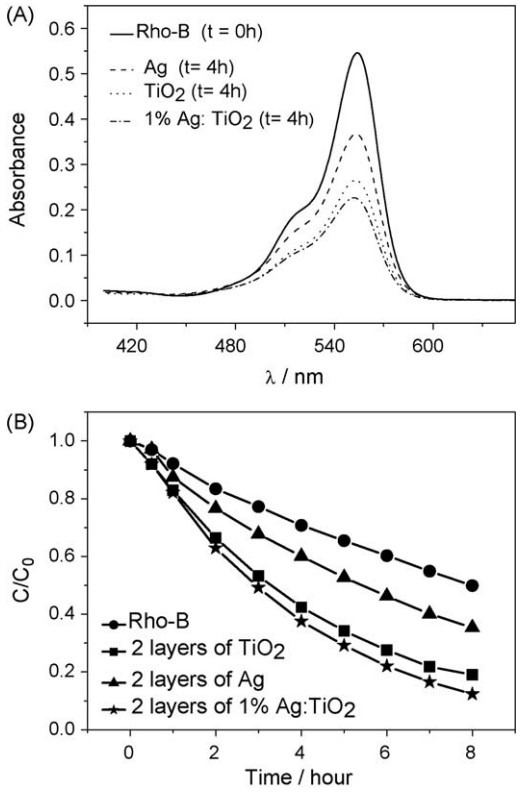

Fig. 11. (A) Absorption spectrum after 4 h photodegradation and (B) degradation profiles of the RhoB solution, in contact with two-layer TiO_2, Ag and 1.0% Ag:TiO_2 films deposited on glass.

Table 2
Photodegradation rate constants for RhoB, Ag, TiO_2, 0.25% Ag:TiO_2, 0.5% Ag:TiO_2 and 1.0% Ag:TiO_2 films.

System	Reaction constant (k')/h^{-1}
Rhodamine B	0.086
Ag film	0.131
TiO_2 film	0.215
1.0% Ag:TiO_2 film	0.263
0.5% Ag:TiO_2 film	0.360
0.25% Ag:TiO_2 film	0.410

law can presented in the form of Eq. (2):

$$v = k'[\mathrm{RhoB}] = -\frac{\mathrm{d}[\mathrm{RhoB}]}{\mathrm{d}t} \quad (2)$$

Putting the initial RhoB concentration equal to $[\mathrm{RhoB}]_0$ and integrating Eq. (2) we have:

$$\ln\frac{[\mathrm{RhoB}]}{[\mathrm{RhoB}]_0} = -k't \quad (3)$$

In accordance with Eq. (3), if $\ln\frac{[\mathrm{RhoB}]}{[\mathrm{RhoB}]_0}$ is plotted as a function of t, a straight line should be obtained, whose slope – k'. A comparative study of the kinetic parameters of the RhoB photodegradation reactions with the two-layer films was thus carried out. The order of reaction was confirmed as one, since the graphs of $\ln\frac{[\mathrm{RhoB}]}{[\mathrm{RhoB}]_0}$ as a function of t showed linear regression coefficients very close to one (R = 0.994). Table 2 shows the rate constants (k') (in h^{-1}) obtained from the photodegradation curves obtained with the two-layer films. It was found that the rate constant for RhoB degradation was higher with the photocatalyst films than in the direct photolysis test. Moreover, when all the prepared films are compared, the rate constants rise in the order: pure Ag < pure TiO_2 < 1.0% Ag:TiO_2 < 0.5% Ag:TiO_2 < 0.25% Ag:TiO_2.

In other words, for the two-layer films (pure Ag, pure TiO_2 and Ag:TiO_2 with different Ag loading content), the decorated film showed the highest photocatalytic efficiency. This increase in the photocatalytic efficiency on loading with Ag can be attributed to the capture of photogenerated negative charges by the Ag centers, causing a reduction in the e^-/h^+ recombination rate, and the possible stabilization of anatase relative to rutile TiO_2, as observed in the XRD patterns for the pure and Ag:TiO_2 powders. Thus, it is probable that in the 1.0% Ag:TiO_2 films, not only did the method of synthesis favor the formation of the desired anatase phase, but the presence of the Ag nanoparticles may also have contributed to the stabilization of this phase.

4. Conclusions

It can be concluded that the synthesis of nanostructured TiO_2 films by the polymeric precursor method was effective for the formation of anatase phase. Moreover, the Ag loading on the TiO_2 films increased their photocatalytic efficiency. This was attributed to the capture of the photogenerated negative charges by the Ag nanoparticles and stabilization of the anatase with respect to the rutile phase. The study of different thicknesses of film deposited on an insulating support showed that for the pure TiO_2 film, the increase in layer thickness is the only factor responsible for the increase in photocatalytic activity. In the case of the 1.0% Ag:TiO_2 film, the reduced rate of recombination, with consequent increase in catalytic efficiency, is related to two effects: electron transfer from TiO_2 to Ag and the increase in the TiO_2 layer thickness. It can be concluded from the results that there is an optimal film thickness, where a balance exists between the effects of electron capture, that increase photoactivity, and the increased opacity of the films due to metallic Ag, that diminishes the photoactivity. This

optimum value was observed in the film with two layers of 0.25% Ag:TiO_2. The comparative study of the kinetic parameters of RhoB photodegradation reactions with the various two-layer films showed that these reactions have first-order kinetics. The values of the rate constants for these reactions in contact with the films were in the order: 0.25% Ag:TiO_2 film > 0.5% Ag:TiO_2 film > 1.0% Ag:TiO_2 film > TiO_2 film > Ag film > direct photolysis. Thus, the Ag decored film showed the highest photocatalytic efficiency.

Acknowledgements

The authors thank CNPq (RHAE and Process 55.5689/2006-9), FAPESP and FINEP for the financial support.

References

[1] M.A. Fox, M.T. Dulay, Chem. Rev. 93 (1993) 341.
[2] N. Venkatachalam, M. Palanichamy, V. Murugesan, Mater. Chem. Phys. 104 (2007) 454.
[3] A. Navrotsky, O.J. Kleppa, J. Am. Ceram. Soc. 50 (1967) 626.
[4] P. Qu, J. Zhao, T. Shen, H. Hidaka, J. Mol. Catal. A: Chem. 129 (1998) 257.
[5] R. Libanori, T.R. Giraldi, E. Longo, E.R. Leite, C. Ribeiro, J. Sol-Gel Sci. Technol. 49 (2009) 95.
[6] H. Wang, Y. Wu, B.Q. Xu, Appl. Catal. B Environ. 59 (2005) 143.
[7] A.L. Linsebigler, G.Q. Lu, T. Yates Jr., Chem. Rev. 95 (1995) 735.
[8] J.R. Garbin, D.M.B.P. Milori, M.L. Simões, W.T.L. da Silva, L. Martin-Neto, Chemosphere 66 (2007) 1692.
[9] F. Sayılkan, M. Asilturk, P. Tatar, N. Kiraz, S. Sener, E. Arpac, H. Sayılkan, Mater. Res. Bull. 43 (2008) 127–134.
[10] B.R. Sankapal, S.D. Sartale, M.C. Lux-Steiner, A. Ennaoui, C. R. Chimie 9 (2006) 702.
[11] C. Ribeiro, C. Vila, J.M.E. Matos, J. Bettini, E. Longo, E.R. Leite, Chem. Eur. J. 13 (2007) 5798.
[12] M. Boudart, G. Djega-Mariadasson, Kinetics of Heterogeneous Reaction, Princeton University Press, Princeton, 1981.
[13] C. Ribeiro, C. Vila, D.B. Stroppa, J. Bettini, V.R. Mastelaro, E. Longo, E.R. Leite, J. Phys. Chem. C 111 (2007) 5871.
[14] C.M. Ronconi, C. Ribeiro, L.O.S. Bulhões, E.C. Pereira, J. Alloys Compd. 466 (2008) 435.
[15] V. Subramanian, E. Wolf, P.V. Kamat, J. Phys. Chem. B 105 (2001) 11439.
[16] G. Colón, M. Maicu, M.C. Hidalgo, J.A. Navío, Appl. Catal. B: Environ. 67 (2006) 41.
[17] B. Xin, Z. Ren, H. Hu, X. Zhang, C. Dong, K. Shi, L. Jing, H. Fu, Appl. Surf. Sci. 252 (2005) 2050.
[18] M. Anpo, M. Takeuchi, J. Catal. 216 (2003) 505.
[19] H.W. Wang, H.C. Lin, C.H. Kuo, Y.L. Cheng, Y.C. Yeh, J. Phys. Chem. Solids 69 (2008) 633.
[20] J. Zhang, M. Li, Z. Feng, J. Chen, C. Li, J. Phys. Chem. B 110 (2006) 927.
[21] J. Yu, J. Xiong, B. Cheng, S. Liu, Appl. Catal. B 60 (2005) 211.
[22] Z.S. Pillai, P.V. Kamat, J. Phys. Chem. B 108 (2004) 945.
[23] M.R. Hoffmann, S.T. Martin, W. Choi, D.W. Bahnemann, Chem. Rev. 95 (1995) 69.
[24] J. Zheng, H. Yu, X. Li, S. Zhang, Appl. Surf. Sci. 254 (2008) 1630.